

000 001 002 003 004 005 006 007 008 009 010 011 012 013 014 015 016 017 018 019 020 021 022 023 024 025 026 027 028 029 030 031 032 033 034 035 036 037 038 039 040 041 042 043 044 045 046 047 048 049 050 051 052 053 **OPENSTAMP: A WATERMARK FOR OPEN-SOURCE LANGUAGE MODELS**

005 **Anonymous authors**

006 Paper under double-blind review

ABSTRACT

With the growing prevalence of large language model (LLM)-generated content, watermarking is considered a promising approach for attributing text to LLMs and distinguishing it from human-written content. A common class of techniques embeds subtle but detectable signals in generated text by modifying token sampling probabilities. However, such methods are unsuitable for open-source models, where users have white-box access and can easily disable watermarking during inference. Existing watermarking methods that support open-source models often rely on complex or compute-intensive training procedures. In this work, we introduce **OpenStamp**, a simple watermarking technique that implants detectable signals into the generated text by modifying just the final projection, or unembedding, layer. Through experiments across two models, we show that **OpenStamp** achieves superior detection performance, with minimal degradation in model capabilities. The implanted watermarking signal is harder to scrub off through post-hoc fine-tuning compared to previous methods, and offers similar robustness against paraphrasing attacks. We have shared our code through an anonymized repository to enable developers to easily watermark their models.

1 INTRODUCTION

Large language models (LLMs) are capable of generating human-like text, which has led to their widespread adoption in various applications (Brown et al., 2020; Chowdhery et al., 2023). As these models become more prevalent, there are looming concerns about potential misuse, such as generating large-scale misinformation (Oviedo-Trespalacios et al., 2023), influencing public opinion (Panditharatne & Giansiracusa, 2023), or orchestrating social engineering attacks (Grbic & Djolovic, 2023). To address these concerns, it is critical to develop methods for distinguishing LLM-generated content from human-written text. Such methods can also be used to attribute the content to its source model, thereby promoting transparency and accountability in LLM use, especially for high-stakes applications. One promising approach to detect model-generated content is to watermark the text by embedding subtle, imperceptible signals into the model’s outputs. To implant such signals, several prominent watermarking techniques either modify the next-token probabilities (Kirchenbauer et al., 2023; Liu & Bu, 2024) or constrain the sampling process during generation (Aaronson, 2023; Kuditipudi et al., 2024). While effective, these decoding-based techniques are incompatible with requirements of open sourcing, where users have full control over the generation process and can easily disable the watermarking logic. This motivates the need for techniques that embed watermarking signals directly into the weights of language models.

Few recent works explore this direction for watermarking open-source LLMs. A notable approach proposes to distill a student model using the outputs of the watermarked teacher model (Gu et al., 2024). However, this method typically requires considerable amounts of training data and computational resources. Another recent study proposes to add Gaussian noise to the bias vector of the final layer, steering the generation towards a fixed set of tokens (Christ et al., 2024), also referred to as the green list in watermarking literature. This scheme may have limited applicability as most LLMs omit bias terms in linear layers (Touvron et al., 2023; Jiang et al., 2023; Radford et al., 2019). Furthermore, recent work shows that watermarks relying on a fixed green list can be reverse-engineered and rendered ineffective (Jovanovic et al., 2024; Rastogi & Pruthi, 2024).

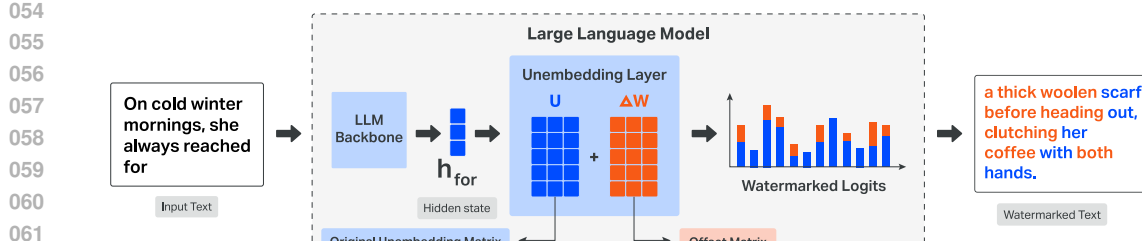


Figure 1: **Overview of our watermarking method.** We add an offset matrix ΔW to the unembedding layer’s weights U to produce **watermark logits** that bias token sampling, favoring tokens with higher watermark logit values. The watermark can be detected using a **log-likelihood ratio (LLR)** based score which measures how much more likely the observed tokens are under the watermarked model compared to the unwatermarked model.

In this work, we introduce **OpenStamp**, a simple approach to watermarking open-source LLMs by modifying the *unembedding layer*¹ weights of the model. We introduce a carefully designed modification to these weights, which bias the logits before generation and thereby implant signals in the generated text. **OpenStamp** is conceptually similar to prior logit-based watermarking approaches (Kirchenbauer et al., 2023; Liu et al., 2024; Liu & Bu, 2024), which influence token selection by adding small, context-dependent biases to the logits at each decoding step. However, an important distinction is that we embed the biasing logic directly into the unembedding layer’s weights. Figure 1 shows a high-level overview of our watermarking method. To detect watermarked text, we compute a length normalized **log-likelihood ratio (LLR)** score, which measures how much more likely the observed tokens are under the watermarked model compared to the unwatermarked model.

OpenStamp offers multiple advantages over prior work. Unlike past approaches (Gu et al., 2024; Xu et al., 2025; Elhassan et al., 2025), it requires no complex training procedures to embed the watermark. Furthermore, unlike Christ et al. (2024), it does not rely on the final layer bias and cannot be trivially removed. Despite its simplicity, **OpenStamp** achieves near-perfect detection ($TPR \geq 99\%$ at 1% FPR) with only minimal degradation in text quality, outperforming other open-source watermarking methods by *over 45 percentage points* in detection accuracy at comparable perplexity levels. Our watermarking method approaches the Pareto frontier defined by prominent decoding-based techniques. Furthermore, our watermarking signal is more difficult to erase via fine-tuning compared to existing approaches and is comparably robust to paraphrasing attacks. We believe that these strengths make our approach a strong candidate for watermarking open-source models. To encourage model developers to watermark their models prior to release, and foster the development of new watermarking techniques for open-source models, we publicly release our code through an anonymized repository: <https://anonymous.4open.science/r/openstamp-78F4/>

2 BACKGROUND AND RELATED WORK

Watermark for Large Language Models. Watermarking techniques for LLMs embed signals in model-generated text that remain imperceptible to human readers but can be algorithmically detected. A common approach alters the decoding process (Kirchenbauer et al., 2023; Liu & Bu, 2024) by boosting a pseudorandom subset of tokens. Detection relies on statistical tests that exploit the resulting skew, for example by comparing the proportion of green tokens against the baseline expected under unwatermarked text. For a comprehensive survey, see Liang et al. (2024).

Watermarks for Open-Source LLMs. In open-source settings, where users control the decoding process, any decoding-time logic can be easily bypassed; hence, the watermarking logic must be embedded directly into the model weights. One approach uses distillation, training a student model on watermarked outputs from a decoding-based watermarked teacher, thereby enabling the student to generate watermarked text natively (Gu et al., 2024). While effective, this method requires substantial computational resources and training data. A reinforcement learning-based framework

¹The unembedding layer is also referred to as the output projection layer or softmax layer.

108 jointly optimizes an LLM and a paired detector to balance detectability and text quality (Xu et al.,
 109 2025). A further line of work embeds a watermark into model weights by jointly fine-tuning LoRA
 110 adapters, optimizing for both coherence and detectability (Elhassan et al., 2025). In addition to re-
 111quiring substantial compute, both methods rely on complex joint optimization objectives that can be
 112challenging to tune.

113 Similar to our work are approaches that embed watermarking logic without requiring any LLM fine-
 114 tuning. One such method introduces a fixed Gaussian perturbation to the final layer’s bias vector,
 115 steering generation towards positively biased tokens (Christ et al., 2024), similar to a fixed green
 116 list (Zhao et al., 2024). However, most LLMs omit bias terms in linear layers (Touvron et al., 2023;
 117 Jiang et al., 2023; Radford et al., 2019), and fixed green-list watermarks are known to be vulnerable
 118 to reverse-engineering attacks (Jovanovic et al., 2024; Rastogi & Pruthi, 2024). GaussMark (Block
 119 et al., 2025) embeds a watermark by adding Gaussian noise to a subset of model weights, and detects
 120 it by analysing how the log-likelihood of a given text changes under the perturbed model. However,
 121 GaussMark can be difficult to embed, as it requires careful selection of the weight subsets and the
 122 noise strength to balance text quality and detectability across models.

123 Despite recent innovations, a key limitation across existing work is the lack of robustness to post-hoc
 124 model modifications. This is a major challenge for watermarking open-source models, which are
 125 often updated through quantization, pruning, merging, or fine-tuning. Gloaguen et al. (2025) find
 126 that no current methods remain detectable after such updates. We present complementary evidence
 127 on this limitation in Section 5.3. Various recent approaches underscore the inherent difficulty of
 128 watermarking in open-source LLMs. Each method exhibits different limitations across several axes:
 129 efficiency of integration, detectability, robustness, and practicality.

130 3 METHODOLOGY

131 **Overview.** This section presents our approach for watermarking language model outputs. We
 132 first introduce the model setup and notation (§3.1), then describe how a simple modification to the
 133 unembedding layer can bias generation towards specific tokens to embed a watermark signal (§3.2).
 134 We outline key desiderata for effective watermarking and show how our design satisfies them (§3.3).
 135 Finally, we describe how to detect the watermark using a log-likelihood ratio based score (§3.4).

136 3.1 PRELIMINARIES

137 Let a language model process a sequence of tokens drawn from a vocabulary \mathcal{V} . Let $x_t \in \mathcal{V}$ denote
 138 the token at generation step t , and let $x_{\leq t} = (x_1, \dots, x_t)$ denote the prefix up to step t . The model
 139 computes a hidden representation $h_t = f(x_{\leq t}) \in \mathbb{R}^d$, where $f : \mathcal{V}^* \rightarrow \mathbb{R}^d$ is the model’s internal
 140 encoding function. The model then produces a logit vector

$$141 v_t = Uh_t \in \mathbb{R}^{|\mathcal{V}|},$$

142 where $U \in \mathbb{R}^{|\mathcal{V}| \times d}$ is the unembedding matrix. The model defines a categorical distribution $p(x_{t+1} |$
 143 $x_{\leq t})$ over the next token by applying a softmax over v_t , where each component $v_t^{(w)}$ corresponds to
 144 the logit value of token $w \in \mathcal{V}$. Watermarking strategies typically modify v_t during generation to
 145 influence the next-token distribution.

146 **KGW Watermarking.** In the KGW watermarking scheme (Kirchenbauer et al., 2023), the logit
 147 modification step is guided by a pseudorandom partition of the vocabulary. At each generation step
 148 t , a pseudorandom function (PRF) selects a subset of tokens $\mathcal{G}_t \subset \mathcal{V}$ called the *green list*, based on
 149 the context $x_{\leq t}$ and a secret key. A parameter γ controls the fraction of tokens in the green list, so
 150 that $|\mathcal{G}_t| = \gamma|\mathcal{V}|$. The logits for tokens in the green list are boosted by a fixed amount $\delta > 0$:

$$151 \hat{v}_t^{(w)} = v_t^{(w)} + \delta \cdot \mathbf{1}\{w \in \mathcal{G}_t\}.$$

152 3.2 WATERMARKING VIA UNEMBEDDING MATRIX MODIFICATION

153 Modifying the unembedding matrix provides a direct mechanism to alter the logit vector produced at
 154 each generation step. Concretely, we define a modified unembedding matrix $\tilde{U} = U + \Delta \mathbf{W}$, where

162 we refer to $\Delta W \in \mathbb{R}^{|\mathcal{V}| \times d}$ as the *offset matrix*. Applying this matrix to a hidden state h_t yields the
 163 modified logit vector $\tilde{v}_t = \tilde{U}h_t = v_t + \Delta W h_t$, where $\Delta W h_t$ is termed *watermark logits*. These
 164 logits bias the output distribution during generation, favoring tokens with higher adjusted scores.
 165 This bias accumulates in the generated text, embedding a detectable watermark signal.

166 Unlike prior approaches that modify arbitrary model weights, altering the unembedding matrix has
 167 interpretable effects: the watermark’s influence on token probabilities is directly determined by the
 168 linear transformation ΔW applied to hidden states. **This linearity allows us to provide a theoretical
 169 justification for why the watermark logits remain stable, as discussed in Appendix J.**
 170

171 **Designing an effective offset matrix.** For our method to be effective, the offset matrix ΔW should
 172 embed a watermark that is:
 173

- 174 • **Detectable** in generated text using algorithmic methods.
- 175 • **Controllable** via hyperparameters that balance detectability and text quality.
- 176 • **Variable** across contexts, avoiding fixed biases that can be reverse-engineered.

177 To meet these desiderata, we now present our design for the offset matrix ΔW .
 178

179 3.3 LINEARIZED GREEN LIST BIASING

180 Inspired by KGW, where a PRF selects a context-dependent green list $\mathcal{G}_t \subset \mathcal{V}$, we model a similar
 181 list-selection mechanism as a composition of two linear transformations. Specifically, we construct
 182 the offset matrix as
 183

$$184 \Delta W = GS,$$

185 where $G \in \mathbb{R}^{|\mathcal{V}| \times L}$ encodes L green lists, and $S \in \mathbb{R}^{L \times d}$ is designed to map the hidden state h_t to a
 186 vector $s = Sh_t \in \mathbb{R}^L$ that approximates a one-hot selector for one of the L green lists. The product
 187 $Gs \in \mathbb{R}^{|\mathcal{V}|}$ then yields watermark logits that closely resembles one of the encoded green lists in G .
 188 Because the hidden state encodes the generation context, this construction parallels KGW’s use of
 189 PRF to tie list selection to context. By maintaining multiple green lists and selecting among them
 190 dynamically through h_t , the method ensures **variability** in the watermark logits across contexts. We
 191 provide supporting evidence of this variability in Appendix G.
 192

193 **Selector Matrix S .** The selector matrix $S \in \mathbb{R}^{L \times d}$ is obtained by solving a ridge regression
 194 problem in which input variables are continuous hidden states and the target outputs are one-hot
 195 vectors representing L pseudo-classes. To build these pseudo-classes, we first extract the hidden
 196 states from the final transformer layer on text sampled from the OpenWebText corpus (Gokaslan &
 197 Cohen, 2019). We then group these hidden states into L clusters using the k -means algorithm. This
 198 gives us a training dataset $\mathcal{D}_{\text{train}} = \{(h_i, e_i)\}_{i=1}^N$, where e_i is the one-hot encoding of the cluster
 199 label for h_i . We then solve:

$$200 \min_S \sum_{(h_i, e_i) \in \mathcal{D}_{\text{train}}} \|Sh_i - e_i\|^2 + \lambda \|S\|_F^2,$$

203 where $\lambda > 0$ is a regularization parameter. Once trained, S can be applied to any hidden state h_t to
 204 produce a soft class indicator $s = Sh_t \approx e_t$. See Appendix B for training details.
 205

206 **Green List Matrix G .** The matrix $G \in \mathbb{R}^{|\mathcal{V}| \times L}$ encodes L candidate green lists as its columns.
 207 For each column $l \in \{1, \dots, L\}$, the corresponding green list $\mathcal{G}_l \subset \mathcal{V}$ is defined by a PRF:
 208

$$209 \mathcal{G}_l = \{i \mid \text{PRF}(\text{seed}, l, i) < \gamma\},$$

210 where `seed` is the secret key shared between watermark generation and detection, and $\text{PRF}(\cdot)$
 211 maps the token index i to a value in $[0, 1]$. Each entry of G is then given by
 212

$$213 G_{i,l} = \delta \cdot \mathbf{1}\{i \in \mathcal{G}_l\}.$$

215 The hyperparameters γ and δ have the same interpretation as in the KGW watermarking scheme,
 offering **controllability** over the watermark’s strength and impact on text quality.

216 **Approximating one-hot selectors.** Since our method operates on continuous hidden states, the
 217 selector matrix S yields soft, continuous selectors instead of exact one-hot vectors. As a result,
 218 multiple green lists can be partially activated at once leading to weaker alignment with the intended
 219 green-list behavior. This effect becomes more pronounced as L grows. Nonetheless, detection
 220 performance remains strong. A detailed analysis of this effect and its influence on detection perfor-
 221 mance is presented in Section 5.5.

222 **3.4 DETECTION VIA LOG-LIKELIHOOD RATIO**

223 To detect the presence of a watermark, we compute a **length-normalized log-likelihood ratio**
 224 (**LLR**) for the given sequence using the watermarked and original model, specifically:

$$227 \quad \text{LLR}(x) = \frac{1}{T} \sum_{t=1}^T \log \frac{p_{\text{wm}}(x_t | x_{<t})}{p_{\text{orig}}(x_t | x_{<t})}, \quad (1)$$

231 where the probabilities are defined via softmax over logits from the original unwatermarked model,
 232 p_{orig} and it's watermarked version, p_{wm} .

233 **Intuition.** The **LLR** score measures how much more likely a given token sequence is under the
 234 watermarked model than under the original model. Because the watermark logits systematically
 235 bias sampling towards certain favored tokens, generations from the watermarked model tend to
 236 accumulate higher LLR values, making the watermark **detectable** in practice. Length normalization
 237 ensures that a single detection threshold can be applied consistently across sequences of different
 238 lengths. A key assumption behind this approach is that unwatermarked text, whether human-written
 239 or generated by other models, is better modeled by the original model than by the watermarked one.
 240 **While the conditional probabilities in Equation 1 formally condition on the full history, detection**
 241 **remains robust using only partial prefixes that exclude the generation prompt. We present empirical**
 242 **evidence in Appendix I that detection performance is largely invariant to prompt inclusion.**

243 Unlike frequency-based detection methods (Kirchenbauer et al., 2023), our **LLR score does not con-**
 244 **stitute** a formal statistical test. The null hypothesis—that the text is unwatermarked—is *composite*,
 245 encompassing human-written and other model-generated text. As noted in Block et al. (2025), this
 246 makes p-value calibration intractable, since the null distribution of the LLR is not well-defined.
 247 **Nevertheless, because the LLR uses the full token probability distribution and naturally captures**
 248 **the mixture of green lists produced by our watermarking method, it preserves signal that frequency-**
 249 **based tests lose by relying only on discrete counts. In Section 5.6, we demonstrate this empirically**
 250 **by comparing our LLR-based detector with ablations that discretize the signal.**

251 **Detection Protocol.** The developer publicly releases a watermarked model with the modified un-
 252 embedding matrix $\tilde{U} = U + \Delta W$, while keeping the original unembedding matrix private. Any
 253 text generated using the public model can be detected using Algorithm 1. This protocol assumes
 254 white-box access to the model weights in order to evaluate log-likelihoods.

256 **Algorithm 1** Watermark Detection via LLR Score

257 **Require:** Sequence $x = (x_1, \dots, x_T)$, LLM backbone $f(\cdot)$, unembedding matrix U , offset matrix
 258 ΔW , threshold τ
 259 **Ensure:** True if x is watermarked; else False
 260 // Extract hidden states from the LLM
 261 1: $(h_1, \dots, h_T) \leftarrow f(x)$
 262 // Compute log-likelihood of sequence under original model
 263 2: $\ell_{\text{orig}} \leftarrow \sum_{t=1}^{T-1} \log \text{softmax}(h_t U^\top)[x_{t+1}]$
 264 // Compute log-likelihood under watermarked model
 265 3: $\ell_{\text{wm}} \leftarrow \sum_{t=1}^{T-1} \log \text{softmax}(h_t (U + \Delta W)^\top)[x_{t+1}]$
 266 // Compute length-normalized LLR score
 267 4: $\text{LLR}(x) \leftarrow (\ell_{\text{wm}} - \ell_{\text{orig}}) / (T - 1)$
 268 5: **return** $(\text{LLR}(x) > \tau)$

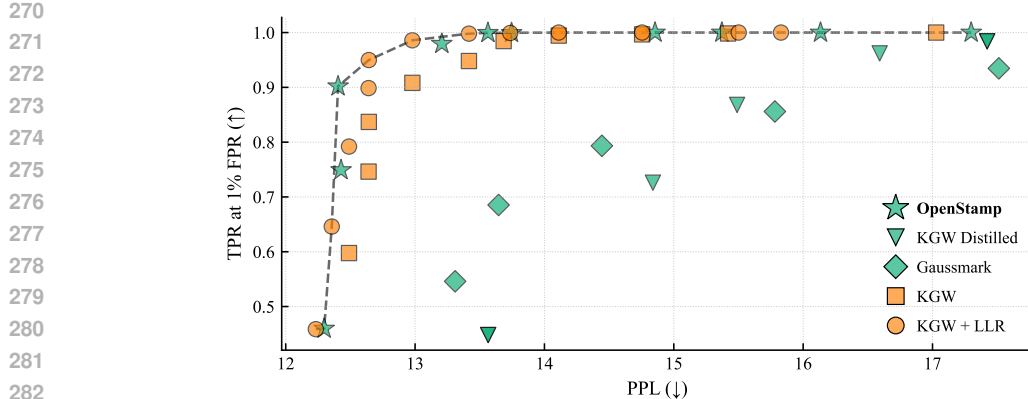


Figure 2: **Trade-off between detectability (TPR at 1% FPR) and text quality (PPL) for various watermarking methods.** KGW + LLR defines the Pareto frontier, establishing an upper bound on detectability at each PPL level. Vanilla KGW performs slightly worse, highlighting the effectiveness of the LLR detection method. Our method, **OpenStamp**, is close to the Pareto frontier and outperforms all open-source compatible methods (shown in green) by a substantial margin.

4 EXPERIMENTAL SETUP

We evaluate our watermarking method across four key dimensions: **(i)** detection performance (§ 5.1), **(ii)** robustness to paraphrasing attacks (§ 5.2), **(iii)** resistance to fine-tuning (§ 5.3) and **(iv)** impact on downstream tasks (§ 5.4). We conduct all experiments along these axes on Llama-2-7B (Touvron et al., 2023). Additional detection performance experiments are conducted on Mistral-7B (Jiang et al., 2023) and presented in Appendix C. Beyond these evaluations, we also provide a deeper analysis of watermarking behavior (§ 5.5) and the LLR detector (§ 5.6).

4.1 BASELINES

We compare our method against two prior open-source-compatible watermarking approaches: GaussMark (Block et al., 2025) and a distilled version of KGW (Gu et al., 2024). We also include standard KGW as a representative of more conventional decoding-based techniques. In addition, we evaluate KGW combined with the LLR-based detector described in Section 3.4, which we regard as an approximate upper bound on detection performance. We omit RL-based watermarking (Xu et al., 2025) because it does not remain robust across different sampling strategies (See Appendix E). We omit Elhassan et al. (2025) because we were unable to train a model that could reliably embed a detectable watermark. Hyperparameters for all methods are provided in Appendix D.

4.2 EVALUATION PROTOCOL

Watermarked Sample Generation. We generate 500 watermarked completions of 200 tokens each, using 50-token prompts sampled from the RealNewsLike subset of C4 (Raffel et al., 2020). The corresponding unwatermarked completions are taken directly from the dataset as the next 200 tokens after each prompt. Detection is performed only on the continuations and excludes the prompts. Watermarked generations are sampled using nucleus sampling with temperature 1.0. To assess generalizability, we also evaluate on prompts drawn from ArXiv (Cohan et al., 2018), BookSum (Kryściński et al., 2022), and Wikipedia (Wikimedia Foundation, 2024).

Metrics. We evaluate two properties: *watermark detectability* and *text quality*. **Detectability** is measured by the AUROC and the true positive rate at a fixed false positive rate of 1% (TPR@1%FPR). In applications such as plagiarism detection, where false positives carry a high cost, maintaining a low FPR is essential, making TPR@1%FPR a particularly relevant metric. **Text quality** is measured by the mean perplexity (PPL) of the watermarked samples, computed using Llama-2-13b as the oracle model. All metrics are averaged over three random seeds, except for KGW Distilled, where only one seed was used due to the high computational cost of distillation.

| Method | ArXiv | | BookSum | | Wikipedia | |
|------------------|-------------|-------------|-------------|-------------|-------------|-------------|
| | TPR@1%FPR | PPL | TPR@1%FPR | PPL | TPR@1%FPR | PPL |
| KGW | 0.99 | 34.1 | 1.00 | 25.1 | 0.97 | 13.7 |
| KGW + LLR | 1.00 | 31.9 | 1.00 | 23.5 | 0.99 | 12.5 |
| KGW Distilled | 0.97 | 40.8 | 0.99 | 30.9 | 0.94 | 15.8 |
| GaussMark | 0.92 | 38.6 | 0.95 | 30.1 | 0.90 | 17.0 |
| OpenStamp | 1.00 | 31.0 | 1.00 | 26.3 | 0.99 | 14.4 |

Table 1: **Watermark detection performance across datasets.** Prompts are sampled from ArXiv, BookSum, and Wikipedia and evaluated on LLaMA-2-7B. Bold values denote the best TPR@1%FPR and lowest PPL per dataset. **KGW** and **KGW + LLR** are decoding-based methods.

5 RESULTS

5.1 DETECTION PERFORMANCE

Figure 2 illustrates the tradeoff between text quality and detectability for various watermarking methods. Each method’s tradeoff curve is generated by varying a method-specific parameter that controls strength of the signal. Open-source methods are shown in green, while decoding-based methods are shown in orange.

OpenStamp achieves near-perfect detection ($TPR \geq 99.9\%$) at a perplexity of approximately 13.6, significantly outperforming Gaussmark and KGW Distilled, which reach only 45-55% TPR at similar PPL levels. The gap between vanilla KGW and the KGW+LLR upper bound highlights the effectiveness of the LLR detection method. As shown in Table 1, our method also outperforms all baselines across other datasets, demonstrating its generalizability. **OpenStamp** shows similar trends across all datasets on Mistral-7B (see Appendix C).

We also assess detection under stricter false-positive constraints, since in many applications even a 1% FPR may be too high. Table 2 reports TPR@0.1% FPR and TPR@0.01% FPR for all methods. **OpenStamp** maintains near-perfect detection at both 0.1% and 0.01% FPR, clearly outperforming GaussMark and KGW Distilled.

| Method | TPR@0.1% FPR | TPR@0.01% FPR | PPL |
|------------------|--------------|---------------|-------------|
| KGW + LLR | 1.00 | 1.00 | 14.8 |
| KGW | 0.99 | 0.99 | 15.5 |
| Gaussmark | 0.74 | 0.74 | 15.7 |
| KGW Distilled | 0.85 | 0.84 | 16.6 |
| OpenStamp | 1.00 | 1.00 | 15.1 |

Table 2: **Detection TPR at stricter FPRs.** **OpenStamp** maintains near-perfect detection performance even at 0.1% and 0.01% FPR, significantly outperforming GaussMark and KGW Distilled.

5.2 ROBUSTNESS TO PARAPHRASING ATTACKS

Paraphrasing attacks pose a major challenge for watermark detection (Krishna et al., 2023; Kirchenbauer et al., 2024). By replacing or rearranging tokens, paraphrasing can dilute the statistical patterns that watermarking methods rely on for detection. To test robustness against such attacks, we use **DIPPER** (Krishna et al., 2023), a paraphrase generation model that allows fine-grained control over *lexical diversity*, a measure of how much the paraphrase’s word choice diverges from the original. We apply DIPPER to watermarked samples with two lexical diversity levels, 20 for lighter edits and 60 for stronger edits. As an upper-bound, we include **UNIGRAM** (Zhao et al., 2024), which uses a static green list and is inherently robust to paraphrasing since its green token set remains fixed regardless of surface form. Note that while **UNIGRAM** is robust to paraphrasing because of its static green list, it is easier to reverse engineer and thus less secure.

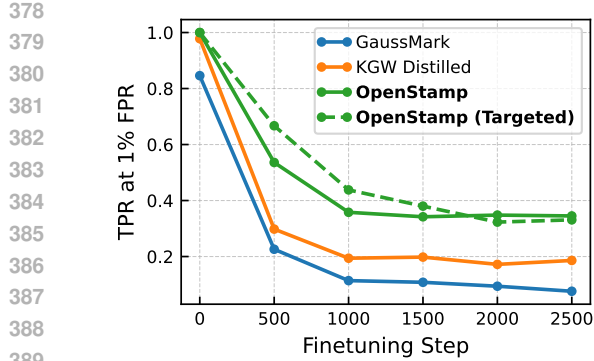


Figure 3: **Detectability under post-hoc fine-tuning.** We report TPR@1%FPR over 2,500 fine-tuning steps. All methods degrade over time, but **OpenStamp** maintains higher detectability compared to GaussMark and KGW Distilled.

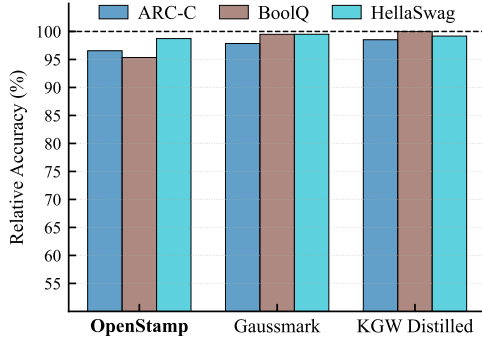


Figure 4: **Relative downstream task accuracy of watermarked models.** Accuracy is shown as a percentage of the unwatermarked baseline (dashed line at 100%). All methods exhibit a degradation in accuracy that is less than 5%.

Table 3 shows that **OpenStamp** achieves the highest TPR@1%FPR at low lexical diversity (20), while GaussMark outperforms at higher diversity (60). We observed a similar trend on Mistral-7B (see Appendix C). Note that a lexical diversity of 20 corresponds to the kind of quick, low-effort edits a human paraphraser might realistically attempt, making it the more practical setting. In contrast, a diversity of 60 is far less realistic, since achieving that level of rewriting would require effort similar to composing the text from scratch.

| Method | LexDiv = 20 | | LexDiv = 60 | |
|------------------|-------------|-------------|-------------|-------------|
| | AUROC | TPR@1%FPR | AUROC | TPR@1%FPR |
| UNIGRAM | 0.99 | 0.87 | 0.97 | 0.56 |
| KGW Distilled | 0.97 | 0.71 | 0.87 | 0.29 |
| GaussMark | 0.96 | 0.63 | 0.92 | 0.47 |
| OpenStamp | 0.99 | 0.89 | 0.88 | 0.45 |

Table 3: **Paraphrasing attack results on LLaMA-2-7B.** LexDiv (Lexical Diversity) measures the degree of paraphrasing; higher LexDiv means stronger paraphrasing. **UNIGRAM** serves as an upper-bound and is expected to remain robust under paraphrastic transformation. Bold indicates top TPR@1%FPR among methods.

5.3 RESISTANCE TO POST-HOC FINE-TUNING

We assess how well open-source compatible watermarking methods can resist post-hoc fine-tuning. Specifically, we simulate an adversary attempting to erase the watermark from model weights by further fine-tuning on OpenWebText (Gokaslan & Cohen, 2019) using LoRA (Hu et al., 2022). Since **OpenStamp** modifies only the unembedding layer, an adversary may leverage this knowledge to perform a more targeted and computationally efficient fine-tuning attack that updates only the unembedding layer. Therefore, we also include this targeted attack in our evaluation. Full experimental details are provided in Appendix F. We measure the TPR@1%FPR after every 500 fine-tuning steps up to 2,500 steps. We discuss more attack setups in Appendix K.

Figure 3 shows that although all watermarking methods degrade over time, **OpenStamp** retains higher detectability than both GaussMark and KGW Distilled. The targeted attack performs similarly to full-model fine-tuning, but serves as a more computationally efficient approach for attempting to erase **OpenStamp**’s watermark.

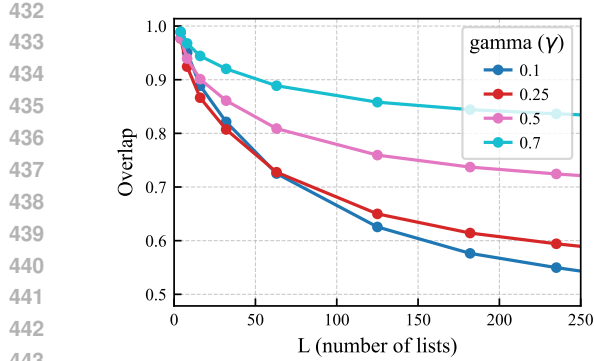


Figure 5: **Green List Token Overlap.** As L increases, the overlap between the top-biased tokens and the intended green list decreases, indicating weakening alignment with the intended green list structure.

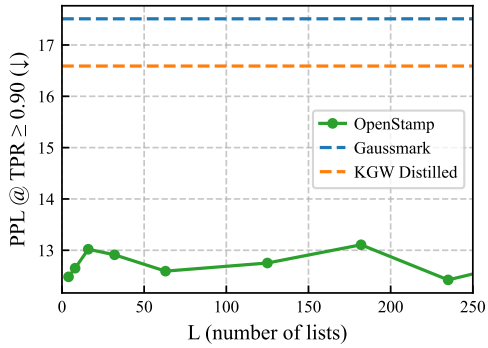


Figure 6: **Detection Performance vs. L .** Minimum PPL to achieve $\text{TPR}@1\% \text{FPR} \geq 0.90$ is reported for different L values. PPL remains stable with growing L and consistently below the GaussMark and KGW Distilled baselines.

5.4 IMPACT ON DOWNSTREAM TASK ACCURACY

Since watermarking strategies alter the output distributions of LLMs, it is essential to ensure that the utility of the underlying model is not significantly compromised. While the results in Figure 2 demonstrate minimal degradation in perplexity, Ajith et al. (2024) find that perplexity measurements cannot reliably predict the performance trade-offs due to watermarking on downstream tasks. Therefore, we further evaluate watermarked models on downstream tasks using the Language Model Evaluation Harness (Gao et al., 2024). We measure the potential performance degradation introduced by watermarking across three benchmarks: ARC-C (Clark et al., 2018), BoolQ (Clark et al., 2019), and HellaSwag (Zellers et al., 2019).

Figure 4 shows the accuracy of various watermarking methods on these tasks, relative to the unwatermarked model. All methods exhibit a degradation in accuracy that is less than 5%, suggesting similar levels of degradation on other downstream tasks.

5.5 ANALYSIS OF WATERMARKING BEHAVIOR

In this section, we study how the hyperparameter L , which represents the number of green lists, influences our watermarking method. We focus on two aspects: (1) the alignment between watermark logits and the green list structure, and (2) the detection performance.

Measuring alignment. We first extract 5,000 hidden states from OpenWebText samples. For each hidden state h , we compute watermark logits $\Delta Wh = GSh$. We measure *overlap*, defined as the fraction of $|\mathcal{G}| = \gamma \cdot |\mathcal{V}|$ tokens with the largest logits in ΔWh that also belong to the intended green list \mathcal{G}_ℓ , where $\ell = \arg \max_i (Sh)_i$. We report overlap for different values of γ and L in Figure 5. As L increases, the overlap decreases, indicating a weakening alignment with the green list structure.

Measuring detection performance. We find the minimum PPL required to achieve $\text{TPR}@1\% \text{FPR} \geq 0.90$ on watermarked samples. A lower PPL threshold indicates a more effective watermark, since it enables reliable detection with less degradation in text quality. We report the PPL threshold for different L values. For comparison, we also report corresponding PPL thresholds for GaussMark and KGW Distilled. Figure 6 shows that PPL remains stable across different L values and consistently below the baseline thresholds.

5.6 LLR VS. DISCRETIZED-SIGNAL DETECTORS

We assess how much the LLR detector benefits from retaining the full continuous watermark signal versus *discretizing* it. For this, we compare the LLR detector against two ablations that discretize the watermark signal: (i) a discrete LLR variant that replaces the soft selector with an argmax before

486 computing likelihoods, and (ii) a binomial count detector that counts the number of selected green
 487 list tokens, following the style of Kirchenbauer et al. (2023). In the discrete LLR variant, the selector
 488 $s = Sh_t$ is collapsed to a single index $\hat{\ell}_t = \arg \max_i s_i$, and the corresponding green list vector
 489 $G_{\hat{\ell}_t} \in \mathbb{R}^{|V|}$ is taken as the discretized signal. The watermarked distribution is then
 490

$$491 \quad p_{\text{wm}}(x_t \mid G_{\hat{\ell}_t}) = \frac{\exp(v_t + G_{\hat{\ell}_t})_{x_t}}{\sum_{w \in V} \exp(v_t + G_{\hat{\ell}_t})_w},$$

$$492$$

$$493$$

494 which the mirrors the numerator in Equation 1 but uses only a single green-list vector, removing all
 495 mixed-list contributions present in the full model. The binomial count detector instead treats green
 496 list membership as a Bernoulli indicator, forming
 497

$$498 \quad Z = \sum_{t=1}^T \mathbf{1}\{x_t \in G_{\hat{\ell}_t}\}, \quad z = \frac{Z - \gamma T}{\sqrt{T\gamma(1-\gamma)}}.$$

$$499$$

$$500$$

501 Table 4 shows TPR at various FPR thresholds for all three detectors. The two discretized-signal
 502 variants recover some watermark signal but they still perform noticeably worse than the LLR de-
 503 tector, indicating that collapsing the mixed green list structure into a single discrete choice loses
 504 information the continuous LLR leverages.
 505

| 507 Method | 508 TPR@1%FPR | 509 TPR@0.1%FPR | 510 TPR@0.001%FPR |
|--------------------|----------------------|------------------------|--------------------------|
| 508 Discrete LLR | 0.96 | 0.82 | 0.79 |
| 509 Binomial Count | 0.86 | 0.51 | 0.50 |
| 510 LLR | 1.00 | 1.00 | 1.00 |

512 Table 4: **Comparing LLR to alternative detectors.** The discretized-signal variants perform worse
 513 than the full LLR detector, indicating that collapsing the mixed green list structure into a single
 514 discrete choice loses useful information.
 515

518 6 LIMITATIONS

520 There are several important limitations of our work. First, detection requires a forward pass through
 521 the model, making it computationally expensive compared to methods that perform statistical tests
 522 on generated text. Second, our method assumes access to token probabilities from the base model.
 523 However, this is a realistic assumption as model owners typically have white-box access to their
 524 models. While our detection algorithm achieves stronger performance, it is not grounded in a sta-
 525 tistical test and thus lacks a probabilistic interpretation, such as confidence levels or false positive
 526 rates, that help quantify detection uncertainty. Finally, the performance of our approach, akin to
 527 existing work, deteriorates under paraphrasing attacks and post-hoc fine-tuning.
 528

529 7 CONCLUSION

531 In this work, we proposed a simple and effective approach for watermarking open-source LLMs by
 532 embedding the watermarking logic directly into the weights of the unembedding layer. This design
 533 enables the watermark to be natively integrated into the models generation process without requiring
 534 decoding-time interventions. We demonstrated that our approach outperforms existing open-source
 535 watermarking methods in detection performance while preserving text quality. Additionally, we
 536 demonstrated that its robustness under paraphrasing and post-hoc model fine-tuning is comparable
 537 to, or surpasses, that of existing methods. Overall, our approach offers strong detectability, control-
 538 lability and can be easily integrated into existing models. Future work could explore more advanced
 539 offset matrix designs to improve robustness against paraphrasing and model modifications such as
 fine-tuning, and to better support the use of detection methods with statistical guarantees.

540 REFERENCES
541

542 Scott Aaronson. 20 - 'Reform' AI Alignment with Scott
543 Aaronson. [https://axrp.net/episode/2023/04/11/](https://axrp.net/episode/2023/04/11/episode-20-reform-ai-alignment-scott-aaronson.html)
544 episode-20-reform-ai-alignment-scott-aaronson.html, 2023. AXRP -
545 The AI X-risk Research Podcast.

546 Anirudh Ajith, Sameer Singh, and Danish Pruthi. Downstream trade-offs of a family of text wa-
547 termarks. In Yaser Al-Onaizan, Mohit Bansal, and Yun-Nung Chen (eds.), *Findings of the Asso-
548 ciation for Computational Linguistics: EMNLP 2024*, pp. 14039–14053, Miami, Florida, USA,
549 2024. Association for Computational Linguistics. doi: 10.18653/v1/2024.findings-emnlp.821.
550 URL <https://aclanthology.org/2024.findings-emnlp.821/>.

551 Adam Block, Alexander Rakhlin, and Ayush Sekhari. Gaussmark: A practical approach for struc-
552 tural watermarking of language models. In *Forty-second International Conference on Machine
553 Learning*, 2025. URL <https://openreview.net/forum?id=YG3DbpAQBF>.

554 Tom Brown, Benjamin Mann, Nick Ryder, Melanie Subbiah, Jared D Kaplan, Prafulla Dhariwal,
555 Arvind Neelakantan, Pranav Shyam, Girish Sastry, Amanda Askell, et al. Language models are
556 few-shot learners. *Advances in neural information processing systems*, 33:1877–1901, 2020.

557 Aakanksha Chowdhery, Sharan Narang, Jacob Devlin, Maarten Bosma, Gaurav Mishra, Adam
558 Roberts, Paul Barham, Hyung Won Chung, Charles Sutton, Sebastian Gehrmann, et al. Palm:
559 Scaling language modeling with pathways. *Journal of Machine Learning Research*, 24(240):
560 1–113, 2023.

561 Miranda Christ, Sam Gunn, Tal Malkin, and Mariana Raykova. Provably robust watermarks for
562 open-source language models. *ArXiv preprint*, abs/2410.18861, 2024. URL <https://arxiv.org/abs/2410.18861>.

563 Christopher Clark, Kenton Lee, Ming-Wei Chang, Tom Kwiatkowski, Michael Collins, and Kristina
564 Toutanova. BoolQ: Exploring the surprising difficulty of natural yes/no questions. In Jill
565 Burstein, Christy Doran, and Thamar Solorio (eds.), *Proceedings of the 2019 Conference of
566 the North American Chapter of the Association for Computational Linguistics: Human Lan-
567 guage Technologies, Volume 1 (Long and Short Papers)*, pp. 2924–2936, Minneapolis, Min-
568 nnesota, June 2019. Association for Computational Linguistics. doi: 10.18653/v1/N19-1300. URL
569 <https://aclanthology.org/N19-1300/>.

570 Peter Clark, Isaac Cowhey, Oren Etzioni, Tushar Khot, Ashish Sabharwal, Carissa Schoenick, and
571 Oyvind Tafjord. Think you have solved question answering? try arc, the ai2 reasoning challenge.
572 *ArXiv preprint*, abs/1803.05457, 2018. URL <https://arxiv.org/abs/1803.05457>.

573 Arman Cohan, Franck Dernoncourt, Doo Soon Kim, Trung Bui, Seokhwan Kim, Walter Chang,
574 and Nazli Goharian. A discourse-aware attention model for abstractive summarization of long
575 documents. In *Proceedings of NAACL*, 2018.

576 Fay Elhassan, Niccolò Ajroldi, Antonio Orvieto, and Jonas Geiping. Can you finetune your binoc-
577 ulars? embedding text watermarks into the weights of large language models. In *The 1st
578 Workshop on GenAI Watermarking*, 2025. URL <https://openreview.net/forum?id=d1v2hkB0Vj>.

579 Leo Gao, Jonathan Tow, Baber Abbasi, Stella Biderman, Sid Black, Anthony DiPofi, Charles Fos-
580 ter, Laurence Golding, Jeffrey Hsu, Alain Le Noac'h, Haonan Li, Kyle McDonell, Niklas Muen-
581 nighoff, Chris Ociepa, Jason Phang, Laria Reynolds, Hailey Schoelkopf, Aviya Skowron, Lin-
582 tang Sutawika, Eric Tang, Anish Thite, Ben Wang, Kevin Wang, and Andy Zou. A framework
583 for few-shot language model evaluation, 2024. URL <https://zenodo.org/records/12608602>.

584 Thibaud Gloaguen, Nikola Jovanović, Robin Staab, and Martin Vechev. Towards watermarking
585 of open-source LLMs. In *The 1st Workshop on GenAI Watermarking*, 2025. URL <https://openreview.net/forum?id=OKjZvLJxOY>.

594 Aaron Gokaslan and Vanya Cohen. Openwebtext corpus. <http://Skylion007.github.io/OpenWebTextCorpus>, 2019.

595

596

597 Dijana Vukovic Grbic and Igor Dujlovic. Social engineering with chatgpt. In *2023 22nd International Symposium INFOTEH-JAHORINA (INFOTEH)*, pp. 1–5. IEEE, 2023.

598

599 Chenchen Gu, Xiang Lisa Li, Percy Liang, and Tatsunori Hashimoto. On the learnability of
600 watermarks for language models. In *The Twelfth International Conference on Learning Representations, ICLR 2024, Vienna, Austria, May 7-11, 2024*. OpenReview.net, 2024. URL
601 <https://openreview.net/forum?id=9k0krNzv1V>.

602

603

604 Edward J. Hu, Yelong Shen, Phillip Wallis, Zeyuan Allen-Zhu, Yuanzhi Li, Shean Wang, Lu Wang,
605 and Weizhu Chen. Lora: Low-rank adaptation of large language models. In *The Tenth International Conference on Learning Representations, ICLR 2022, Virtual Event, April 25-29, 2022*.
606 OpenReview.net, 2022. URL <https://openreview.net/forum?id=nZeVKeeFYf9>.

607

608 Albert Q. Jiang, Alexandre Sablayrolles, Arthur Mensch, Chris Bamford, Devendra Singh Chap-
609 lot, Diego de las Casas, Florian Bressand, Gianna Lengyel, Guillaume Lample, Lucile Saulnier,
610 Lélio Renard Lavaud, Marie-Anne Lachaux, Pierre Stock, Teven Le Scao, Thibaut Lavril,
611 Thomas Wang, Timothée Lacroix, and William El Sayed. Mistral 7b, 2023. URL <https://arxiv.org/abs/2310.06825>.

612

613

614 Nikola Jovanovic, Robin Staab, and Martin T. Vechev. Watermark stealing in large language mod-
615 els. In *Forty-first International Conference on Machine Learning, ICML 2024, Vienna, Austria,
616 July 21-27, 2024*. OpenReview.net, 2024. URL <https://openreview.net/forum?id=Wp054bnPq9>.

617

618 John Kirchenbauer, Jonas Geiping, Yuxin Wen, Jonathan Katz, Ian Miers, and Tom Goldstein.
619 A watermark for large language models. In Andreas Krause, Emma Brunskill, Kyunghyun
620 Cho, Barbara Engelhardt, Sivan Sabato, and Jonathan Scarlett (eds.), *International Confer-
621 ence on Machine Learning, ICML 2023, 23-29 July 2023, Honolulu, Hawaii, USA*, volume
622 202 of *Proceedings of Machine Learning Research*, pp. 17061–17084. PMLR, 2023. URL
623 <https://proceedings.mlr.press/v202/kirchenbauer23a.html>.

624

625 John Kirchenbauer, Jonas Geiping, Yuxin Wen, Manli Shu, Khalid Saifullah, Kezhi Kong, Kasun
626 Fernando, Aniruddha Saha, Micah Goldblum, and Tom Goldstein. On the reliability of water-
627 marks for large language models. In *The Twelfth International Conference on Learning Repre-
628 sentations, 2024*. URL <https://openreview.net/forum?id=DEJIDCmWOz>.

629

630 Kalpesh Krishna, Yixiao Song, Marzena Karpinska, John Wieting, and Mohit Iyyer. Paraphras-
631 ing evades detectors of ai-generated text, but retrieval is an effective defense. In Alice Oh,
632 Tristan Naumann, Amir Globerson, Kate Saenko, Moritz Hardt, and Sergey Levine (eds.),
633 *Advances in Neural Information Processing Systems 36: Annual Conference on Neural In-
634 formation Processing Systems 2023, NeurIPS 2023, New Orleans, LA, USA, December 10 -
635 16, 2023*, 2023. URL http://papers.nips.cc/paper_files/paper/2023/hash/575c450013d0e99e4b0ecf82bd1afaa4-Abstract-Conference.html.

636

637 Wojciech Kryściński, Bryan McCann, Caiming Xiong, and Richard Socher. Booksum: A collection
638 of datasets for long-form narrative summarization. In *Proceedings of the 60th Annual Meeting of
the Association for Computational Linguistics (Volume 1: Long Papers)*, 2022.

639

640 Rohith Kuditipudi, John Thickstun, Tatsunori Hashimoto, and Percy Liang. Robust distortion-free
641 watermarks for language models. *Transactions on Machine Learning Research*, 2024. ISSN
642 2835-8856. URL <https://openreview.net/forum?id=FpaCL1MO2C>.

643

644 Yuqing Liang, Jiancheng Xiao, Wensheng Gan, and Philip S. Yu. Watermarking techniques for large
645 language models: A survey, 2024. URL <https://arxiv.org/abs/2409.00089>.

646

647 Aiwei Liu, Leyi Pan, Xuming Hu, Shiao Meng, and Lijie Wen. A semantic invariant robust water-
648 mark for large language models. In *The Twelfth International Conference on Learning Represen-
649 tations, 2024*. URL <https://openreview.net/forum?id=6p8lpe4Mnf>.

648 Yepeng Liu and Yuheng Bu. Adaptive text watermark for large language models. In *Forty-first*
 649 *International Conference on Machine Learning, ICML 2024, Vienna, Austria, July 21-27, 2024*.
 650 OpenReview.net, 2024. URL <https://openreview.net/forum?id=7emOSb5Ufx>.
 651

652 OpenAI. Chatgpt. <https://chat.openai.com/>, 2025. Large language model; accessed
 653 2025-09-01.

654 Oscar Oviedo-Trespalacios, Amy E Peden, Thomas Cole-Hunter, Arianna Costantini, Milad
 655 Haghani, JE Rod, Sage Kelly, Helma Torkamaan, Amina Tariq, James David Albert Newton,
 656 et al. The risks of using chatgpt to obtain common safety-related information and advice. *Safety*
 657 *science*, 167:106244, 2023.

658 Mekela Panditharatne and Noah Giansiracusa. How ai puts elections at risk—and the needed safe-
 659 guards. *Brennan Center for Justice*. Retrieved July, 22:2023, 2023.

660

661 F. Pedregosa, G. Varoquaux, A. Gramfort, V. Michel, B. Thirion, O. Grisel, M. Blondel, P. Pretten-
 662 hofer, R. Weiss, V. Dubourg, J. Vanderplas, A. Passos, D. Cournapeau, M. Brucher, M. Perrot, and
 663 E. Duchesnay. Scikit-learn: Machine learning in Python. *Journal of Machine Learning Research*,
 664 12:2825–2830, 2011.

665 Guilherme Penedo, Hynek Kydlíček, Anton Lozhkov, Margaret Mitchell, Colin A Raffel, Leandro
 666 Von Werra, Thomas Wolf, et al. The fineweb datasets: Decanting the web for the finest text data
 667 at scale. *Advances in Neural Information Processing Systems*, 37:30811–30849, 2024.

668

669 Alec Radford, Jeff Wu, Rewon Child, David Luan, Dario Amodei, and Ilya Sutskever.
 670 Language models are unsupervised multitask learners. 2019. URL <https://api.semanticscholar.org/CorpusID:160025533>.

671

672 Colin Raffel, Noam Shazeer, Adam Roberts, Katherine Lee, Sharan Narang, Michael Matena, Yanqi
 673 Zhou, Wei Li, and Peter J. Liu. Exploring the limits of transfer learning with a unified text-to-
 674 text transformer. *J. Mach. Learn. Res.*, 21:140:1–140:67, 2020. URL <http://jmlr.org/papers/v21/20-074.html>.

675

676 Saksham Rastogi and Danish Pruthi. Revisiting the robustness of watermarking to paraphrasing
 677 attacks. In *Proceedings of the 2024 Conference on Empirical Methods in Natural Language Pro-
 678 cessing*, pp. 18100–18110, Miami, Florida, USA, November 2024. Association for Computational
 679 Linguistics. doi: 10.18653/v1/2024.emnlp-main.1005. URL <https://aclanthology.org/2024.emnlp-main.1005/>.

680

681 Hugo Touvron, Louis Martin, Kevin Stone, Peter Albert, Amjad Almahairi, Yasmine Babaei, Niko-
 682 lay Bashlykov, Soumya Batra, Prajjwal Bhargava, Shruti Bhosale, et al. Llama 2: Open foun-
 683 dation and fine-tuned chat models. *ArXiv preprint*, abs/2307.09288, 2023. URL <https://arxiv.org/abs/2307.09288>.

684

685 Sean Welleck, Ilia Kulikov, Stephen Roller, Emily Dinan, Kyunghyun Cho, and Jason Weston.
 686 Neural text generation with unlikelihood training. In *International Conference on Learning Rep-
 687 resentations*, 2020. URL <https://openreview.net/forum?id=SJeYe0Ntvh>.

688

689 Wikimedia Foundation. Wikipedia Dumps. <https://dumps.wikimedia.org>, 2024. Ac-
 690 cessed: 2024-12-01.

691

692 Xiaojun Xu, Yuanshun Yao, and Yang Liu. Learning to watermark LLM-generated text via re-
 693 inforcement learning. In *The 1st Workshop on GenAI Watermarking*, 2025. URL <https://openreview.net/forum?id=dT1CMiEOdk>.

694

695 Rowan Zellers, Ari Holtzman, Yonatan Bisk, Ali Farhadi, and Yejin Choi. Hellaswag: Can a ma-
 696 chine really finish your sentence? *arXiv preprint arXiv:1905.07830*, 2019.

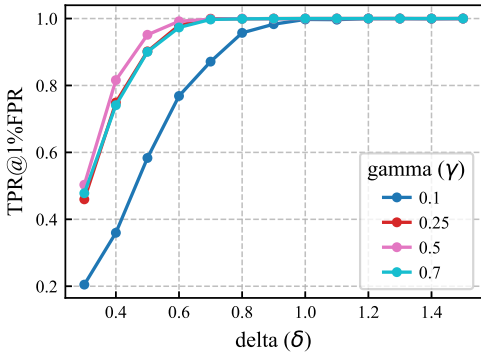
697

698 Xuandong Zhao, Prabhanjan Vijendra Ananth, Lei Li, and Yu-Xiang Wang. Provable robust wa-
 699 termarking for ai-generated text. In *The Twelfth International Conference on Learning Rep-
 700 resentations, ICLR 2024, Vienna, Austria, May 7-11, 2024*. OpenReview.net, 2024. URL
 701 <https://openreview.net/forum?id=SsmT8aO45L>.

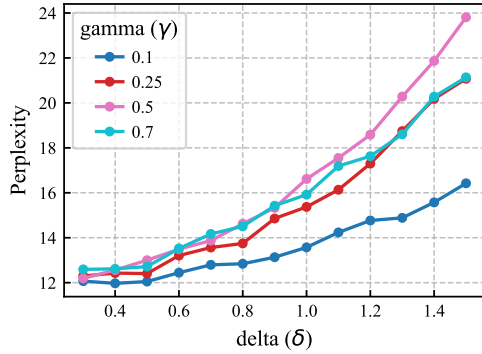
APPENDICES

A EFFECT OF VARYING γ AND δ .

We measure the detectability and text quality of watermarked samples generated using different values of γ and δ . The results, shown in Figures 7a and 7b, indicate the trade-off between detectability and distortion as we vary these parameters.



(a) **Effect of γ and δ on detectability.** TPR@1%FPR vs. δ for various γ values.



(b) **Effect of γ and δ on text quality.** Perplexity vs. δ across the same γ settings, measured using Llama-2-13b.

B TRAINING THE SELECTOR MATRIX

We train the selector projection matrix S to classify hidden state vectors into L distinct classes, where L is an hyperparameter. To obtain the training data, we collect 1.5 million hidden states from the model’s final layer by passing OpenWebText (Gokaslan & Cohen, 2019) sequences of maximum length 512 through the model. We apply MiniBatchKMeans from `scikit-learn` (Pedregosa et al., 2011) to group these hidden states into L clusters. Clusters with fewer than 10 hidden states are discarded to ensure sufficient representation. We set the ridge regression regularization parameter λ to 10^{-3} throughout our experiments.

C RESULTS ON MISTRAL-7B

We present additional results on the Mistral-7b model across two axes: **detection performance** and **robustness to paraphrasing attacks**. We compare our method against GaussMark.

Hyperparameters. For `OpenStamp`, we set the hyperparameters to $\delta = 1.0$, $\gamma = 0.25$, and $L = 203$. For GaussMark, we add noise to the up projection weights of the 20th decoder block with $\sigma = 0.005$.

Detection Performance. We evaluate the detection performance of `OpenStamp` on prompts sampled from the same datasets described in Section 4.2. Table 5 shows that `OpenStamp` achieves a TPR@1%FPR of 1.00 across all datasets, with significantly lower perplexity (PPL) compared to the GaussMark baseline.

Robustness to Paraphrasing Attacks. To evaluate robustness to paraphrasing attacks, we use the same paraphrasing setup as described in Section 5.2. Table 6 shows that `OpenStamp` reports a higher TPR@1%FPR than GaussMark at both levels of lexical diversity.

| Dataset | Metric | GaussMark | OpenStamp |
|--------------|-----------|-----------|-------------|
| RealNewsLike | TPR@1%FPR | 0.77 | 0.99 |
| | PPL | 15.3 | 14.1 |
| ArXiv | TPR@1%FPR | 0.78 | 1.00 |
| | PPL | 34.1 | 26.6 |
| BookSum | TPR@1%FPR | 0.94 | 1.00 |
| | PPL | 26.9 | 24.6 |
| Wikipedia | TPR@1%FPR | 0.68 | 0.99 |
| | PPL | 14.4 | 13.1 |

Table 5: **Watermark detection performance for Mistral-7b.** Prompts are sampled from RealNewsLike, ArXiv, BookSum, and Wikipedia, evaluated on Mistral-7B. Bold values indicate the best TPR@1%FPR and lowest PPL per dataset.

| Method | LexDiv = 20 | | LexDiv = 60 | |
|------------------|-------------|-------------|-------------|-------------|
| | AUROC | TPR@1%FPR | AUROC | TPR@1%FPR |
| GaussMark | 0.92 | 0.41 | 0.88 | 0.24 |
| OpenStamp | 0.98 | 0.78 | 0.87 | 0.30 |

Table 6: **Paraphrasing attack results on Mistral-7B.** Bold indicates top TPR@1%FPR among methods.

D HYPERPARAMETER DETAILS FOR WATERMARKING METHODS

This section details the experimental setup and hyperparameters used across all experiments. For each watermarking method, we perform a parameter sweep to generate the plot in Figure 2. For other evaluations, such as robustness to paraphrasing attacks (§ 5.2), downstream task accuracy (§ 5.4), and resistance to post-hoc fine-tuning (§ 5.3), we select a single representative configuration from each method.

OpenStamp We encode $L = 235$ green lists, each containing a fraction $\gamma = 0.25$ of green tokens. The strength parameter δ is swept over the range $\{0.3, 0.4, \dots, 1.2\}$ for the Pareto evaluation. For all other experiments, we select $\delta = 1.0$ as the representative configuration.

GaussMark Baseline For GaussMark Block et al. (2025), we perturbed the MLP up-projection weights in a single decoder block using Gaussian noise. For Llama-2-7b, the 27th decoder block was used with $\sigma \in \{0.025, 0.03, 0.035, 0.04, 0.045\}$. The configuration $\sigma = 0.04$ is chosen for all other experiments.

KGW Distilled Baseline We trained several logit-distilled KGW variants Gu et al. (2024) using a green list fraction $\gamma = 0.25$ and strength values $\delta \in \{1.0, 1.25, 1.5, 1.75, 2.0\}$ for the Pareto plot. The distilled model with $\delta = 2.0$ was selected for all other evaluations.

KGW Decoding-Time Watermark We used the decoding-time KGW watermark Kirchenbauer et al. (2023), which biases the model’s logits during generation without requiring any parameter modification. We set $k = 1$, which is the token context length used by the PRF to generate green lists. We fixed the green list fraction $\gamma = 0.25$ and swept the bias strength $\delta \in \{0.7, 0.8, \dots, 2.0\}$ to populate the Pareto frontier. [For Table 2 and Table 1, we selected \$\delta = 1.5\$.](#)

KGW + LLR Detection Variant We additionally evaluated KGW with an LLR-based detection strategy (Section 3.4) to simulate a white-box detection setting. The hyperparameters were fixed at $\gamma = 0.25$ and $\delta \in \{0.5, 0.6, \dots, 1.7\}$ for the Pareto evaluation. [For Table 2 and Table 1, we selected \$\delta = 1.4\$.](#)

810 E PRACTICAL CHALLENGES WITH RL-BASED WATERMARKING
811

812 We attempted to implement the RL-based watermarking method from Xu et al. (2025). However,
813 the trained RL model was unable to generate detectable watermarks when the text was generated using
814 multinomial sampling, and it could only embed a strong watermark when sampling with greedy
815 decoding. This is not practical for real-world applications, as greedy decoding often produces repetitive
816 and low-quality text.

817 We quantify repetition using seq-rep-3, the proportion of duplicate 3-grams in a sequence (Welleck
818 et al., 2020):

$$819 \quad 1 - \frac{\# \text{ of unique 3-grams}}{\# \text{ of 3-grams}}$$

820 We report mean seq-rep-3 across watermarked samples for both RL watermarking and our
821 method under greedy and multinomial (temperature = 1.0) decoding, along with TPR@1%FPR.
822 Results in table Table 7 show that while greedy decoding makes RL watermarks detectable, it also
823 causes severe repetition, limiting practicality. In contrast, our method preserves low repetition while
824 maintaining strong detectability across both decoding strategies.

| 827 Method | 828 Multinomial | | 829 Greedy | |
|----------------------|------------------------|----------------------|----------------------|----------------------|
| | 830 TPR@1%FPR | 831 seq-rep-3 | 832 TPR@1%FPR | 833 seq-rep-3 |
| 834 RL Watermarking | 0.25 | 0.03 | 0.99 | 0.58 |
| 835 OpenStamp | 1.0 | 0.03 | 1.0 | 0.03 |

836 Table 7: **Detectability (TPR@1%FPR) and text repetition (mean seq-rep-3) for RL watermarking and OpenStamp under multinomial and greedy decoding.** While RL watermarking
837 achieves high detectability with greedy decoding, it causes severe repetition, whereas **OpenStamp**
838 maintains both strong detectability and low repetition across settings.

839 F FINE-TUNING SETUP DETAILS

840 We fine-tune all models on OpenWebText. We follow a setup similar to Gloaguen et al. (2025): we
841 use a batch size of 64 with 512 tokens per input and a learning rate of $2e^{-5}$. We use the Adafactor
842 optimizer with cosine learning rate decay and

843 linear warmup for the first 500 steps. For LoRA Hu et al. (2022), we set the rank to 16, the scaling
844 factor (alpha) to 32, and the dropout rate to 0.1. For our general fine tuning attack we fine-tune all the
845 internal linear layers of the transformer blocks. For the targeted fine-tuning attack on **OpenStamp**
846 , we perform full fine-tuning (i.e., without LoRA) on only the unembedding layer.

847 G EFFECT OF L ON LOGIT VARIABILITY.

848 We study how increasing L affects the variability of watermark logits across different contexts.
849 With more green lists available, hidden states can be assigned to a greater number of distinct green
850 lists. This increases the diversity of tokens favored by the watermark, making it less predictable and
851 more robust to reverse-engineering attacks. We measure variability by computing the mean Jaccard
852 similarity between the sets of token indices corresponding to the top $\gamma|V|$ components of watermark
853 logits across hidden states. We evaluate this metric for different values of L and γ . Lower similarity
854 implies greater variability in the watermark logits. As shown in Figure 8, mean similarity decreases
855 with increasing L , though the decline plateaus for large L , reflecting diminishing marginal gains in
856 variability.

857 H LLM USAGE

858 ChatGPT (OpenAI, 2025) was used to assist with typesetting (e.g., equations, tables) and for minor
859 language editing (grammar and conciseness). All outputs were reviewed and validated by the
860 authors.

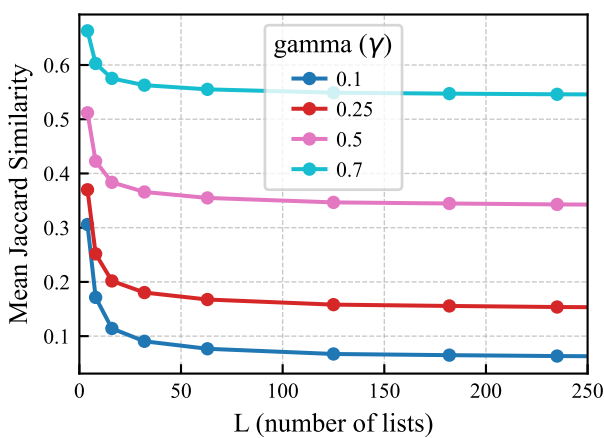


Figure 8: **Variability in Watermark Logits.** As L increases, the mean Jaccard similarity between different top-biased token sets decreases, indicating greater variability in watermark logits across different contexts.

I PROMPT INDEPENDENCE OF WATERMARK DETECTION

To explain why our detection method works without the original prompt, we compare per-token LLR scores on watermarked and unwatermarked text, with and without the prompt. As shown in Figures 9a and 9b, the scores are largely consistent across settings, diverging only slightly at the start of generation. This suggests that hidden states—and thus green-list selections—depend mainly on the immediate local context rather than the initial prompt, allowing effective watermark detection even when the prompt is unavailable.

J BOUNDEDNESS OF WATERMARK LOGITS

At each step t , the watermark logits is defined as $\Delta v_t = \Delta GSh_t$, where h_t is the final-layer hidden state. We assume that hidden states are bounded in norm, which is a reasonable assumption due to the normalization typically applied to final-layer hidden states in Transformer architectures. Furthermore, the selector matrix S is a fixed linear operator with a constant finite operator norm ($\|S\|_{op} = C_S$), and the green list matrix G , containing entries in $\{0, \delta\}$, has an operator norm strictly proportional to δ (i.e., $\|G\|_{op} \leq \delta C_G$). Combining these properties yields a strict upper bound on the perturbation:

$$\|\Delta v_t\|_2 \leq \|G\|_{op} \|S\|_{op} \|h_t\|_2 \leq \delta \cdot (C_G C_S C_h).$$

This implies that the watermark logits are finitely bounded and can be controlled via δ .

K ADDITIONAL ATTACK SETUPS

Here we explore several attack setups aimed at erasing the watermark from the weights or recovering the green list assignments.

K.1 REINITIALIZING AND RETRAINING THE UNEMBEDDING LAYER

An adversary may attempt to completely remove the watermark by reinitializing the unembedding layer and relearning the mapping from hidden states to token logits to restore the model’s capability to generate fluent text. However, restoring this capability is non-trivial since model developers train LLMs on large curated datasets and rely on complex pretraining and post-training pipelines.

To illustrate this difficulty, we reinitialized the unembedding layer and retrained only that layer on FineWeb (Penedo et al., 2024). Table 8 reports perplexity after 2,500 and 25,000 training steps.

918

919

920

921

922

923

924

925

926

927

928

929

930

931

932

933

934

935

936

937

938

939

940

941

942

943

944

945

946

947

948

949

950

951

952

953

954

955

956

957

958

959

960

961

962

963

964

965

966

967

968

969

970

971

Japan is less than two years away from making a fundamental change in its legal system, by allowing jury trials. Under the new system, average citizens will work alongside judges to issue verdicts in many criminal cases. As Yur

iko Yamane explains, it has left some Japanese landlords scrambling for new tenants. <0x0A> Several years of delays in concluding a trade deal between Japan and the European Union caused EU leaders to postpone a summit with Prime Minister Abe that was scheduled for earlier this month. But EU negotiators say the delay may be temporary—and that Japan is finally ready to meet economic pressures. <0x0A> Eurosystem heads promise on overdue rate hike in motion, for it. <0x0A> Monetary Policy of the European Central Bank: An Assessment of the Policy Framework—Impact on Bank Credit Conditions and Bank Loans to SMEs. <0x0A> Local governments across Japan are being hit hard by reduced demand for public works construction from companies tied to foreign businesses. Tokyo's bling nervous about out of control astroturfing from all sides. <0x0A> Nipped in the bud at last, cryptocurrency

iko Yamane explains, it has left some Japanese landlords scrambling for new tenants. <0x0A> Several years of delays in concluding a trade deal between Japan and the European Union caused EU leaders to postpone a summit with Prime Minister Abe that was scheduled for earlier this month. But EU negotiators say the delay may be temporary—and that Japan is finally ready to meet economic pressures. <0x0A> Eurosystem heads promise on overdue rate hike in motion, for it. <0x0A> Monetary Policy of the European Central Bank: An Assessment of the Policy Framework—Impact on Bank Credit Conditions and Bank Loans to SMEs. <0x0A> Local governments across Japan are being hit hard by reduced demand for public works construction from companies tied to foreign businesses. Tokyo's bling nervous about out of control astroturfing from all sides. <0x0A> Nipped in the bud at last, cryptocurrency

(a) Watermarked Text

Japan is less than two years away from making a fundamental change in its legal system, by allowing jury trials. Under the new system, average citizens will work alongside judges to issue verdicts in many criminal cases. As Yur

iko Nagano reports from Tokyo, the greatest hurdle to the experiment is expected to be persuading Japanese citizens to participate. <0x0A> In Japan, as in most Asian countries, judges alone make decisions in trials. But starting in 2009, juries will be participating in Japanese courts, under what is called a "saibanin" system. <0x0A> The new system has not yet been confirmed. At first, it will be tested for three years. And it will be limited in scope. Juries will only be used in certain criminal cases, involving serious crimes such as murder. <0x0A> Robert Precht, a U.S. defense lawyer and legal scholar at the University of Montana, is helping Japanese judges, prosecutors, defense lawyers and citizens to implement the change. He spoke to journalists in Tokyo on Thursday. <0x0A> "The saibanin system and these other reforms are intended to transform

iko Nagano reports from Tokyo, the greatest hurdle to the experiment is expected to be persuading Japanese citizens to participate. <0x0A> In Japan, as in most Asian countries, judges alone make decisions in trials. But starting in 2009, juries will be participating in Japanese courts, under what is called a "saibanin" system. <0x0A> The new system has not yet been confirmed. At first, it will be tested for three years. And it will be limited in scope. Juries will only be used in certain criminal cases, involving serious crimes such as murder. <0x0A> Robert Precht, a U.S. defense lawyer and legal scholar at the University of Montana, is helping Japanese judges, prosecutors, defense lawyers and citizens to implement the change. He spoke to journalists in Tokyo on Thursday. <0x0A> "The saibanin system and these other reforms are intended to transform

(b) Unwatermarked Text

Figure 9: **Prompt Independence of Watermark Detection.** Per-token LLR scores for (a) watermarked and (b) unwatermarked text, computed with and without the prompt. The red highlight indicates tokens with a negative score whereas the green highlight indicates tokens with a positive score. The text in blue is the prompt. Scores are similar in both settings, indicating that detection is robust to the absence of the original prompt.

972 Even with substantial retraining, perplexity remained far worse than the original model’s, showing
 973 that recovering quality is non-trivial and making this attack computationally costly.
 974

| Condition | PPL |
|---------------------------------|---------|
| Watermarked Baseline | 15.1 |
| After 2500 Steps (80M tokens) | 78529.4 |
| After 25000 Steps (800M tokens) | 351.7 |

981 Table 8: **Perplexity after retraining a reinitialized unembedding layer.**
 982
 983

984 K.2 INVERSION ATTACK VIA RECONSTRUCTING THE SELECTOR MATRIX

985 We evaluate a plausible inversion attack based on the intuition that an adversary might try to reconstruct
 986 the selector matrix S and then reverse-engineer each cluster’s green list. In practice, this attack
 987 is particularly challenging because key details—such as the number of clusters L , the k-means
 988 initialization seed, and the dataset used to extract hidden states—are kept private by the model provider.
 989

990 Even if the attacker guesses L , reproducing the original hidden-state-to-cluster assignments is highly
 991 sensitive to both the k-means seed and the underlying dataset. To illustrate this sensitivity, we con-
 992 struct selector matrices with the same L using different datasets (OpenWebText vs. FineWeb) and
 993 different initialization seeds. We then generate a test set of hidden states from RealNewsLike sam-
 994 ples and compute cluster assignments under each variant of the selector matrix. Agreement between
 995 assignments is measured using Adjusted Rand Index (ARI) and Normalized Mutual Information
 996 (NMI). As shown in Table 9, cluster assignments vary across datasets and seeds. This variability
 997 suggests that reconstructing the original selector matrix is challenging, providing inherent robust-
 998 ness against this class of inversion attacks.
 999

| Condition | ARI | NMI |
|--------------------------|------|------|
| Different Dataset | 0.44 | 0.65 |
| Different Seed | 0.46 | 0.67 |
| Different Dataset & Seed | 0.37 | 0.63 |

1000
 1001 Table 9: **Agreement between cluster assignments from different selector matrices.** The ARI and
 1002 NMI scores indicate moderate agreement, showing that reconstructing the original selector matrix
 1003 is challenging even with knowledge of L .
 1004
 1005
 1006
 1007
 1008
 1009
 1010
 1011
 1012
 1013
 1014
 1015
 1016
 1017
 1018
 1019
 1020
 1021
 1022
 1023
 1024
 1025